The sodium channel β-subunit SCN3b modulates the kinetics of SCN5a and is expressed heterogeneously in sheep heart

Ahmed I. Fahmi, Manoj Patel*, Edward B. Stevens†, Abigail L. Fowden‡, James Edward John III*, Kevin Lee†, Robert Pinnock†, Kevin Morgan, Antony P. Jackson and Jamie I. Vandenberg

*Department of Biochemistry, University of Cambridge, Downing Site, Cambridge CB2 1QW, UK, *Department of Internal Medicine, Cardiovascular Division, University of Virginia Health Science Center, Charlottesville, VA 22908, USA, †Pfizer Global Research and Development, Cambridge University Forvie Site, Robinson Way, Cambridge CB2 2QB, UK and ‡Department of Physiology, University of Cambridge, Downing Site, Cambridge CB2 3EG, UK*

(Received 8 May 2001; accepted after revision 14 August 2001)

1. Cardiac sodium channels are composed of a pore-forming α-subunit, SCN5a, and one or more auxiliary β-subunits. The aim of this study was to investigate the role of the recently discovered member of the β-subunit family, SCN3b, in the heart.

2. Northern blot and Western blot studies show that SCN3b is highly expressed in the ventricles and Purkinje fibres but not in atrial tissue. This is in contrast to the uniform expression of SCN1b throughout the heart.

3. Co-expression of SCN3b with the cardiac-specific α-subunit SCN5a in *Xenopus* oocytes resulted in a threefold increase in the level of functional sodium channel expression, similar to that observed when SCN1b was co-expressed with SCN5a. These results suggest that both SCN1b and SCN3b improve the efficiency with which the mature channel is targeted to the plasma membrane.

4. When measured in cell-attached oocyte macropatches, SCN3b caused a significant depolarising shift in the half-voltage of steady-state inactivation compared to SCN5a alone or SCN5a + SCN1b. The half-voltage of steady-state activation was not significantly different between SCN5a alone and SCN5a + SCN3b or SCN5a + SCN1b.

5. The rates of inactivation for SCN5a co-expressed with either subunit were not significantly different from that for SCN5a alone. However, recovery from inactivation at −90 mV was significantly faster for SCN5a + SCN1b compared to SCN5a + SCN3b, and both were significantly faster than SCN5a alone.

6. Thus, SCN1b and SCN3b have distinctive effects on the kinetics of activation and inactivation, which, in combination with the different patterns of expression of SCN3b and SCN1b, could have important consequences for the integrated electrical activity of the intact heart.

Voltage-dependent sodium channels are responsible for the rapid upstroke of the action potential in atrial and ventricular myocytes (Marban *et al.* 1998). Even minor alterations in sodium channel function can have profound effects on excitability (Priori, 2000); for example, the gain-of-function mutations in *SCN5a* (the gene that encodes the α-subunit of the main cardiac sodium channel) are a cause of long-QT syndrome (LQTS; Wang *et al.* 1995), and loss-of-function mutations in *SCN5a* are a cause of Brugada syndrome (Chen *et al.* 1998) and Lenegre disease (Schott *et al.* 1999).

The sodium channel is a multi-subunit protein complex composed of a single large α-subunit along with smaller additional β-subunits (Catterall, 2000). There are at least three different β-subunit genes, *SCN1b* (Isom *et al.* 1992; Makita *et al.* 1994), *SCN2b* (Isom *et al.* 1995) and *SCN3b* (Morgan *et al.* 2000), all of which are expressed widely in

excitable tissues. The functional role of sodium channel β-subunits in the heart is still uncertain (Marban *et al.* 1998). However, most studies have found that co-expression of SCN1b with SCN5a causes a small but significant acceleration in the recovery from inactivation (Nuss *et al.* 1995; Baroudi *et al.* 2000). Furthermore, co-expression of SCN1b leads to an increased level of current density, suggesting that it may increase the efficiency with which the mature channel is targeted to the plasma membrane (Nuss *et al.* 1995; Qu *et al.* 1995). The role of SCN2b is more controversial, although recent studies suggest that they do not have a significant functional role in the heart (Malhotra *et al.* 2001). The role in the heart of the recently discovered third member of this family, SCN3b (Morgan *et al.* 2000), has not yet been examined. SCN3b is expressed widely in excitable and non-excitable tissues (Stevens *et al.* 2001). The predicted tertiary structure of SCN3b is similar to that of SCN1b (Morgan *et al.* 2000). Furthermore, SCN3b, like SCN1b, affects both the steady-state inactivation and accelerates the kinetics of inactivation of the neuronal-specific SCN2a sodium channels (Morgan *et al.* 2000) and skeletal muscle-specific SCN4a sodium channels (Stevens *et al.* 2001).

The aim of this study was to investigate the distribution of SCN1b and SCN3b in the heart and to compare the effects of SCN1b and SCN3b on the kinetics of SCN5a when co-expressed in *Xenopus* oocytes. SCN1b and SCN3b have distinct patterns of expression in the heart, with SCN1b expressed throughout the heart, whereas SCN3b is expressed in the ventricles and Purkinje fibres but is absent from the atria. Both subunits affect the level of expression of functional sodium channels when expressed in *Xenopus* oocytes. SCN1b and SCN3b, however, have significantly different effects on the kinetics of SCN5a when co-expressed in *Xenopus* oocytes.

METHODS

Molecular studies were performed on sheep heart tissue to enable us to extract enough protein and RNA from different regions of individual hearts to examine for heterogeneity of expression. All procedures were carried out in accordance with the UK Animals (Scientific Procedures) Act 1986. Hearts were excised from adult ewes that had been killed by an overdose of sodium pentobarbitone (200 mg kg^{-1} I.V.), and dissected into the left and right atria, and left and right ventricles. The basal left ventricular free wall was dissected into epicardial and endocardial sections. Purkinje fibres were dissected from the endocardial surface of the left and right ventricles. RNA was extracted by passage through RNeasy columns (Qiagen, Crawley, UK).

cDNA probes were synthesised by RT-PCR from sheep left ventricle using standard protocols (Wong *et al.* 1999). Sheep cDNA probes to exons 3–4 of *SCN3b*, exons 5–6 of *SCN1b* and exons 15–16 of *SCN5a* were 88, 85 and 91 % homologous, respectively, to the corresponding human sequences. The SCN1b and SCN3b cDNA probes had < 10 % sequence similarity and showed no cross-reactivity on Northern blots. Probes were labelled with [^{32}P]CTP using the multiprime labelling kit (Amersham, UK). Northern blots were hybridised at 58 °C, washed with 2 × saline–sodium citrate buffer (SSC)–1 % SDS (56 °C) for 15 min, followed by 0.5 × SSC–1 % SDS (56 °C) twice for 10 min and exposed to X-ray film. All Northern blots were exposed for 2 days at −80 °C using intensifying screens. Autoradiograms were scanned and quantified using NIH image software (Wong *et al.* 1999).

Membrane proteins were extracted by homogenising tissue on ice in the presence of pepstatin A, 1 μg ml^{-1}; leupeptin, 1 μg ml^{-1}; aprotinin, 1 μg ml^{-1}; pefabloc SC, 0.2 mM; benzamidine, 0.1 μg ml^{-1}; Calpain inhibitor I, 8 μg ml^{-1}; Calpain inhibitor II, 8 μg ml^{-1} (all from Sigma, Poole, UK). Samples were centrifuged at 1000 *g* for 10 min to remove nuclei and debris. The supernatant was then centrifuged twice at 40 000 *g* for 10 min at 4 °C and the pellet re-suspended in Tris-EDTA buffer and 2 % Triton X-100, stored on ice for 1 h and then centrifuged at 13 000 *g* for 10 min to remove insoluble material.

The SCN1b rabbit polyclonal antibody (a kind gift from L. Isom, University of Michigan) was raised against the peptide sequence corresponding to the initial 18 amino acids of the rat β1 sequence, GGCVEVDSETEAVYGMTF, as described previously (Isom *et al.* 1992). The SCN3b rabbit polyclonal antibody was raised against the peptide FEFEAHRPFVKTTRC, corresponding to residues 126–140 of the rat SCN3b sequence, a region that has no sequence homology to the SCN1b sequence. Furthermore, Blast searches with the SCN1b and SCN3b peptide sequences only identified the parent protein in both cases. The pan-specific sodium channel antibody, SP19, was purchased from Alomone Labs (Jerusalem, Israel).

Membrane proteins were separated on 3–8 % SDS-polyacrylamide gels and transferred to polyvinylidene difluoride membranes. Membranes were incubated with primary antibody (1:300 for SP19, 1:800 for anti-SCN1b, 1:500 for SCN3b), washed, and incubated with horseradish peroxidase-conjugated secondary antibody (Abcam, Cambridge, UK) at a dilution of 1:5000–1:10 000. Detection was carried out using the SuperSignal West Dura Substrate Detection kit (Pierce, Rockford, IL, USA). Membranes were exposed for 2–5 min, depending on the intensity of the signal, and densitometric analysis was performed as for the Northern blots.

Capped cRNAs for human SCN5a (kindly donated by A. George Jr, Vanderbilt University; Gellens *et al.* 1992), rat SCN1b (kindly donated by L. Isom, University of Michigan; Isom *et al.* 1992) and rat SCN3b (Morgan *et al.* 2000) were transcribed *in vitro* from linearised cDNAs, using the mMessage mMachine kit (Ambion, Austin, TX, USA). Preparation of *Xenopus* oocytes was performed as described previously (Patel *et al.* 2000; Stevens *et al.* 2001). Two-electrode voltage-clamp recordings were performed using microelectrodes with resistances between 0.2 and 0.5 MΩ and filled with 3 M KCl. Cell-attached macropatch recordings were performed using 0.5–1.0 MΩ electrodes filled with normal Tyrode solution (containing 150 mM NaCl), as described previously (Patel *et al.* 2000). Currents were sampled at 33 kHz and low-pass filtered at 5 kHz using a 3900A Dagan headstage amplifier (Dagan, Minneapolis, MN, USA).

All data were analysed using pCLAMP software (Axon instruments, Foster City, CA, USA). Two-electrode voltage-clamp recordings were leak subtracted offline, assuming a linear leak between −100 and +20 mV, using the pCLAMP leak subtraction routine. Patch recordings were capacitance and leak subtracted by subtracting records obtained where the probability of opening (P_o) for sodium channels is low. For the activation protocol, depolarisations from −50 to +50 mV were used for subtraction; for the steady-state inactivation, currents elicited at the most depolarised potential were used for subtraction, and for recovery from inactivation, the trace generated at the shortest recovery time, and which elicited no active sodium current, was used for subtraction. To improve the signal:noise ratio for patch recordings, an average of at least two, and usually three, traces for each protocol were recorded in each patch. Steady-state activation and inactivation curves were fitted

with the Boltzmann equation: $g = 1/(1 + \exp((V - V_{½})/k))$, where g is conductance, $V_{½}$ is voltage of half-maximal activation/inactivation and k is the slope factor.

Statistical significance was assessed by ANOVA, and paired and unpaired t tests were performed with Student-Newman-Keuls test. A P value of < 0.05 was considered significant.

RESULTS

Typical examples of Northern blots probed for SCN1b, SCN3b and SCN5a are illustrated in Fig. 1*A*. SCN3b was expressed most abundantly in the left ventricle, with moderate expression in the right ventricle and Purkinje fibres, but was not expressed in the atria. Furthermore, there was a higher level of expression of SCN3b mRNA in the endocardial region compared to the epicardial region (Fig. 1*B*). In contrast, SCN1b was expressed uniformly throughout the heart. The relative levels of expression of SCN1b, SCN3b and SCN5a, normalised to that of glyceraldehyde 3-phosphate dehydrogenase (GAPDH), are summarised in Fig. 1*C* and *D*.

Typical examples of Western blots incubated with SP19, SCN1b and SCN3b antibodies are illustrated in Fig. 2*A–C* and the relative levels of expression of the different subunits in different chambers are summarised in Fig. 2*D*. SP19 detected three bands in the region 220–270 kDa. No bands were seen when the membranes were pre-incubated with the peptide antigen, suggesting that all three bands were likely to be sodium channels. Treatment of samples with *N*-glycosidase F indicated that the upper band was a glycoslyated form, but the minor band at about 220 kDa appeared to be a distinct subunit (data not shown). The level of α-subunit expression was greater in the left ventricle and atria than

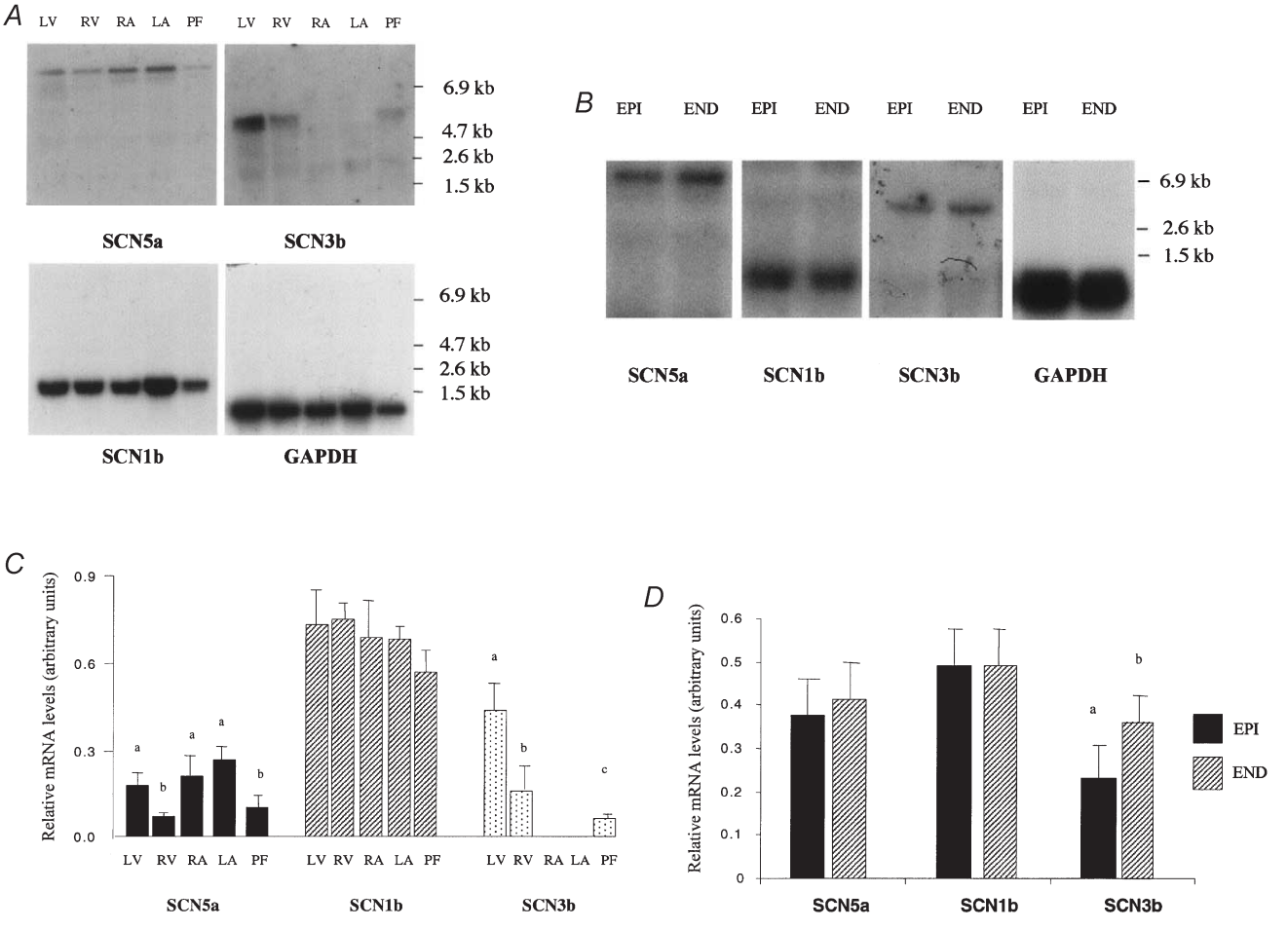

Figure 1. Northern blot analyses of samples of tissue from different regions of the heart

A, Northern blot analysis of left ventricle (LV), right ventricle (RV), left atrium (LA), right atrium (RA) and Purkinje fibre (PF) samples. *B*, Northern blot analysis of LV epicardial (EPI) and LV endocardial (END) samples. In both *A* and *B* a single blot was successively probed for SCN5a (~8.5 kb), SCN3b (~5 kb), SCN1b (~1.5 kb) and glyceraldehyde 3-phosphate dehydrogenase (GAPDH; ~1.0 kb). Size markers are indicated to the right. The mean (± S.E.M., $n = 3$) levels of expression of the α- and β-subunits in different chambers and different regions of the LV are shown in *C* and *D*, respectively. All values were normalised to the level of GAPDH expression. Different superscript letters indicate significant differences between groups for each mRNA species ($P < 0.05$, ANOVA).

Table 1. Steady-state activation and inactivation for SCN5a alone, SCN5a + SCN1b and SCN5a + SCN3b using the cell-attached macropatch (Patch) and two-electrode voltage-clamp (2EVC) methods

	$V_{½}$ (mV)			k (mV)		
	SCN5a	SCN5a + SCN1b	SCN5a + SCN3b	SCN5a	SCN5a + SCN1b	SCN5 + SCN3b
Inactivation						
Patch	−96.1 ± 3.1 (6)	−95.5 ± 0.8 (4)	−85.2 ± 2.6 (6)*	4.5 ± 0.5 (6)	4.7 ± 0.4 (4)	4.2 ± 0.2 (6)
2EVC	−65.3 ± 0.9 (6)	−65.9 ± 0.7 (6)	−60.7 ± 1.3 (6)*	6.5 ± 0.3 (6)	6.7 ± 0.3 (6)	5.9 ± 0.3 (6)
Activation						
Patch	−25.3 ± 2.0 (9)	−20.7 ± 1.8 (6)	−23.7 ± 1.8 (7)	8.0 ± 0.4 (9)	6.4 ± 0.4 (6)	9.6 ± 0.3 (7)*
2EVC	−18.6 ± 4.2 (5)	−23.3 ± 2.0 (5)	−21.3 ± 2.4 (5)	6.0 ± 1.1 (5)	−8.6 ± 0.4 (5)	−7.7 ± 0.7 (5)

Values of n are given in parentheses. *$P < 0.05$ compared to other values in the group

in the right ventricle and atria (see Fig. 2*D*). The SCN1b antibody detected a major band at about ~45 kDa that was expressed at similar levels in all regions. Anti-SCN3b detected two closely spaced bands at about 45–50 kDa. These bands were prominent in the left ventricle and right ventricle, but were absent in atrial tissue samples. Neither band was present when membranes were incubated with the pre-immune serum, suggesting that both bands were likely to be isoforms of SCN3b.

The clearest effect of co-expressing SCN1b or SCN3b with SCN5a in *Xenopus* oocytes was an increase in peak current amplitude from 4.9 ± 1.0 μA (SCN5a alone; $n = 8$) to 14.2 ± 2.3 μA (SCN5a + SCN1b; $n = 7$) or 15.2 ± 2.1 μA (SCN5a + SCN3b, $n = 8$) for depolarisation steps to −40 mV (Fig. 3) when measured 3 days after injection. The kinetics of SCN5a ± SCN1b or SCN3b were determined in oocytes where current amplitudes were < 2 μA (either by injecting oocytes with smaller amounts of RNA and/or studying oocytes 1–2 days after injection). The data for steady-state activation and inactivation from the two-electrode voltage-clamp experiments are summarised in Table 1. Even with small currents, however, it is difficult to obtain sufficiently rapid voltage control to make accurate kinetic measurements. To enable better voltage control, we

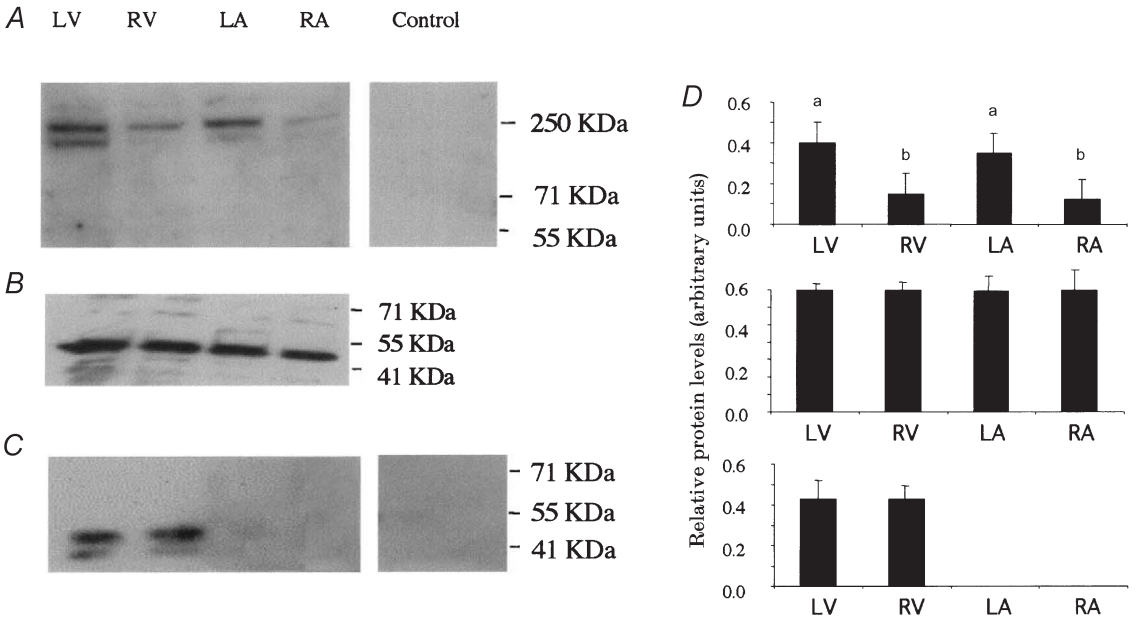

Figure 2. Western blot analyses of sodium channel α-subunits in different chambers of the heart

Western blot analysis of sodium channel α-subunits (~220–270 kDa) (*A*), SCN1b (~45 kDa) (*B*), and SCN3b (~45–50 kDa) (*C*) in different chambers of the heart. Size markers are indicated to the right. A 60 μg sample of protein was loaded per lane. The lane to the right in *A* (Control) shows the result following preincubation with peptide antigen (SP19). The lane to the right in *C* (Control) shows no immunoreactivity when incubated with the preimmune serum. We did not have preimmune serum or control antigen for the SCN1b antiserum; however, this is a very well characterised antibody (e.g. see Isom *et al.* 1992). *D*, the mean ± S.E.M. ($n = 3$) levels of expression of the α- and β-subunits in different chambers of the heart. Different superscript letters indicate significant differences between groups for each subunit ($P < 0.05$, ANOVA).

measured currents in cell-attached patches (see Fig. 4). In cell-attached patches, the steady-state activation parameters were not significantly different from those recorded using the two-electrode voltage-clamp technique (see Table 1). Conversely, the inactivation parameters for SCN5a ± β-subunits were significantly shifted in a hyperpolarised direction compared to the two-electrode voltage-clamp data (see Table 1). The relative differences in the half-voltages of inactivation for SCN5a compared to SCN5a + SCN1b or SCN5a + SCN3b were, however, similar for the two-electrode voltage-clamp and macropatch methods.

The time course of current decay for the macropatch data was voltage dependent and was reasonably well fitted by a single exponential. The rates of current decay were similar for SCN5a alone, and SCN5a co-expressed with either SCN3b or SCN1b with time constants ranging from 2 ms at −30 mV to 0.3 ms at +40 mV. Furthermore, the time to peak current was similar for all groups, ranging from 1.2 ms at −30 mV to 0.3 ms at +40 mV.

The clearest kinetic differences following co-expression of β-subunits was on the rates of recovery from inactivation. Following a 200 ms pre-pulse to −20 mV, the recovery from inactivation at −110 mV for both SCN5a + SCN1b and SCN5a + SCN3b was slightly faster than for SCN5a alone, as measured using either the two-electrode voltage-clamp or cell-attached patch method (see Table 2). The recovery from inactivation at −90 mV was more complex, exhibiting two distinct components (see Fig. 5) in the patch data. The clear distinction between the fast and slow components, however, was not as apparent in the two-electrode voltage-clamp recordings (data not shown). SCN5a + SCN1b channels recovered most rapidly (time for half-recovery from inactivation, $t_{½} = 1.6 \pm 0.9$ ms, $n = 5$). SCN5a alone and SCN5a + SCN3b had similar times for half-recovery from inactivation (see Table 2); however, there were clearly significant differences in the slow phase of recovery from inactivation between SCN5a alone and SCN5a + SCN3b (see Fig. 5).

Table 2. Recovery from inactivation for SCN5a alone, SCN5a + SCN1b and SCN5a + SCN1b

	$t_{½}$ (ms)		
	SCN5a	SCN5a + SCN1b	SCN5a + SCN3b
−90 mV			
Patch	9.3 ± 1.4 (6)	1.6 ± 0.9 (5)*	8.9 ± 1.6 (4)
2ECV	14 ± 0.4 (6)*	8 ± 0.3 (6)	8 ± 0.5 (6)
−110/−120 mV †			
Patch	2.5 ± 0.1 (4)	2.2 ± 0.2 (4)	2.3 ± 0.1 (4)
2ECV	6 ± 0.1 (6)*	4 ± 0.1 (6)	4 ± 0.1 (6)

$t_{½}$, time for half-recovery from inactivation. † 2EVC data were obtained at −110 mV and the patch data at −120 mV. Values of n are given in parentheses. * $P < 0.05$ compared to other values in the group.

DISCUSSION

Understanding the molecular basis of cardiac sodium channel activity has been of major interest in recent years, as mutations in the α-subunit, SCN5a, are associated with a range of arrhythmia syndromes including LQTS, Brugada syndrome and Lenegre disease (Priori, 2000). In addition to the pore-forming α-subunit, SCN5a, multiple β-subunits are expressed in the heart, including SCN1b, SCN2b and the recently described SCN3b subunit (Morgan *et al.* 2000; Stevens *et al.* 2001).

In this study, we have shown that SCN3b is expressed heterogeneously in the heart; the highest level of expression was seen in the ventricles, moderate expression in the Purkinje fibres and minimal expression was detected in the atria, either at the mRNA (see Fig. 1) or at the protein level (see Fig. 2). Furthermore, there was a small gradient of mRNA expression across the left ventricular wall (endocardial > epicardial). The bands on

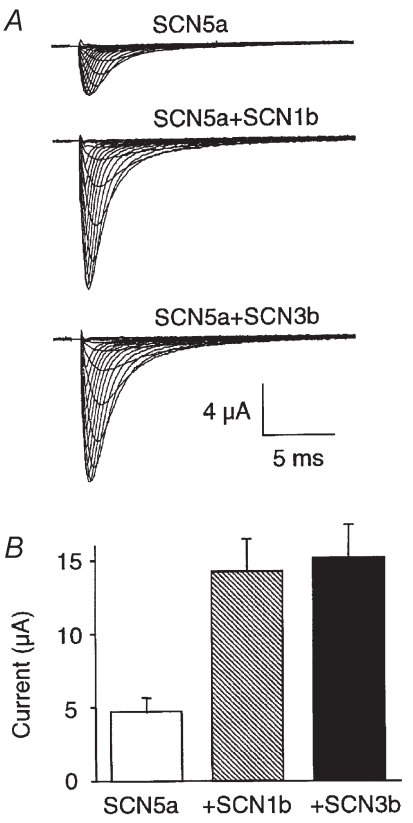

Figure 3. Currents recorded from *Xenopus* oocytes for the sodium channel α- and β-subunits

A, typical families of ion currents recorded from *Xenopus* oocytes during step depolarisations from −100 mV to −80 mV to +10 mV (in 5 mV steps) for SCN5a alone (top), SCN5a + SCN1b (middle) and SCN5a + SCN3b (bottom). *B*, mean ± S.E.M. current amplitude at −40 mV recorded from *Xenopus* oocytes 3 days after injection with ~3 ng SCN5a ± 30 ng SCN1b or SCN3b.

Western blots for SCN3b (45–50 kDa) were significantly larger than the predicted molecular weight, which is consistent with the protein being glycosylated. The two bands on the Western blot could be due to different levels of glycosylation or alternative spliced isoforms. The presence of two bands on the Northern blot are consistent with there being alternative splicing. Furthermore, we have not detected any other SCN3b-like sequences in the human genome sequence, which suggests that the two bands are unlikely to represent different but homologous proteins.

In contrast to the heterogeneous distribution of SCN3b, SCN1b was uniformly expressed in all regions of the heart. A single prominent band was observed on the Western blots for SCN1b at ∼45 kDa, similar to that reported previously (Sutkowski & Catterall, 1990). Similarly, we only detected a single band on Northern blots, at ∼1.5 kb. The results from the distribution data suggest that atrial sodium channels are exclusively SCN5a + SCN1b, whereas ventricular sodium channels are composed of either SCN5a + SCN3b or SCN5a + SCN1b.

One of the most obvious effects of co-expressing β-subunits with SCN5a in *Xenopus* oocytes was a much higher current amplitude (Fig. 3, see also Nuss *et al.* 1995; Qu *et al.* 1995). There are conflicting reports on the extent to which β-subunits increase the current amplitude of SCN2a subunits (Isom *et al.* 1992; Morgan *et al.* 2000). Hence it is possible that the efficiency with which β-subunits increase current amplitude may vary with different α-subunit isoforms. The simplest explanation for this effect is that SCN1b and SCN3b increase the expression of channels at the plasma membrane. Partially assembled multi-subunit membrane proteins are often retained in the endoplasmic reticulum by distinct quality control mechanisms (Ellgard *et al.* 1999). In some cases, for example the nicotinic acetylcholine receptor (Blount *et al.* 1990), membrane proteins can only enter the forward secretory pathway following binding of auxiliary subunits that hide or otherwise override the retention

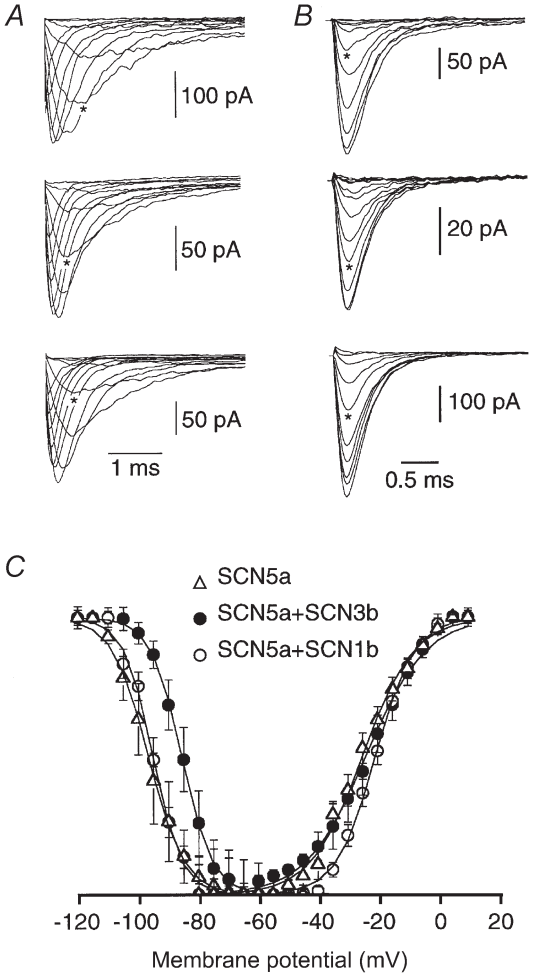

Figure 4. Typical examples of ion currents recorded from *Xenopus* oocyte cell-attached macropatches

A, patches were depolarised from −120 mV to −80 mV to +40 mV (in 5 mV intervals; not all traces are shown) for SCN5a (top), SCN5a + SCN3b (middle) and SCN5a + SCN1b (bottom). The asterisks indicate −30 mV traces. *B*, step depolarisations to −20 mV following a prepulse to voltages in the range −120 to −60 mV (in 5 mV intervals; not all traces are shown). The asterisks indicate −95 mV traces. Each set of traces represents the average of three recordings from the same macropatch. *C*, voltage dependence of steady-state inactivation and activation for SCN5a (△), SCN5a + SCN1b (○) and SCN5a + SCN3b (●). The smooth lines are Boltzmann functions fitted to the averaged data.

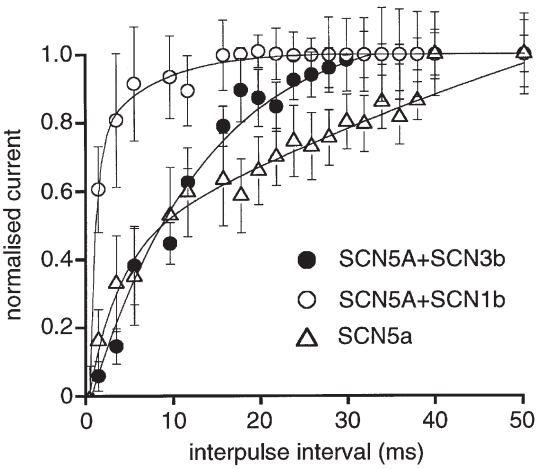

Figure 5. Recovery from inactivation of the different sodium channel subunits

Recovery from inactivation for SCN5a (△), SCN5a + SCN1b (○) and SCN5a + SCN3b (●) at −90 mV. Patches were held at −120 mV and then depolarised to −10 mV for 200 ms and repolarised to −90 mV for times varying from 1 to 400 ms, before being depolarised to −10 mV again. Current magnitudes were normalised to the value recorded after a 400 ms interpulse interval.

signals exposed in the unassembled protein. It is tempting to suggest that sodium channel β-subunits act in a similar manner.

The different levels of expression of the different β-subunits in different regions of the heart are not likely to explain the different levels of functional sodium channel density in Purkinje fibres, and atrial and ventricular myocytes (Purkinje fibres > atrial myocytes > ventricular myocytes; Li & Shrier, 2001). Rather, the Northern and Western blot results suggest that any differences in levels of functional sodium channels in different chambers of the heart are more likely to be due to differences in the level of SCN5a expression (see Figs 1 and 2).

There are very few studies that have compared the kinetics of sodium channel activity in atrial and ventricular myocytes under identical conditions. In a recent study, Li & Shrier (2001) reported a 10.1 mV depolarising shift in the half-voltage for steady-state inactivation in guinea-pig ventricular myocytes compared to that of guinea-pig atrial myocytes. This is similar to the 9.7 mV depolarising shift in the half-voltage for steady-state inactivation we found for SCN5a + SCN3b compared to SCN5a + SCN1b. Our results are therefore consistent with atrial myocytes being predominantly composed of SCN5a + SCN1b, whereas ventricular myocytes are composed of SCN5a + SCN3b as well as SCN5a + SCN1b. In the same study, Li & Shrier (2001) reported that the half-voltages for steady-state activation were slightly more negative for atrial compared to ventricular sodium channels. This is in contrast to what we would have anticipated if the ventricular channels were SCN5a + SCN3b compared to SCN5a + SCN1b in atria, as we found no significant differences in the half-voltage for steady-state activation for SCN5a co-expressed with SCN3b or SCN1b. However, in both studies the differences were significantly smaller (−3.0 to +5.6 mV) than the changes observed for steady-state inactivation (+9.7 to +10.1 mV).

There have been few studies of regional differences in sodium channel activity within the ventricle. Watanabe *et al.* (1985) showed that the action potential upstroke velocity was faster in the subendocardium than in the subepicardium, suggesting that there is a higher density of functional sodium channels in the subendocardium compared to subepicardium. Since SCN3b improves the efficiency with which mature channels reach the plasma membrane, a higher expression of SCN3b in endocardial compared to epicardial regions could explain the findings of Watanabe *et al.* (1985). More recently, Sakmann *et al.* (2000) reported a heterogeneous distribution of the persistent sodium current in guinea-pig ventricular myocytes. However, the heterogeneity in SCN3b expression that we saw (endocardium > epicardium) is different from that reported by Sakmann *et al.* for the persistent sodium current (mid-myocardial cells < epicardium ≈ endocardium). It is therefore unlikely that differences in SCN3b expression could account for differences in the distribution of the late persistent sodium current.

The rate of recovery from inactivation was significantly faster for SCN5a + SCN1b (see also Nuss *et al.* 1995; Baroudi *et al.* 2000) compared to SCN5a + SCN3b or SCN5a alone at −90 mV (i.e. a potential close to the resting membrane potential of cardiac myocytes; see Fig. 5). The combination of SCN5a + SCN1b would therefore be expected to permit faster reactivation than would SCN5a + SCN3b, thereby leading to a shorter refractory period. If the majority of SCN5a subunits co-assemble with either SCN1b or SCN3b and there is a simple competition between SCN1b and SCN3b, then it is possible that the distribution of sodium channel subunits could contribute to the normal heterogeneity of refractoriness in the heart.

Loss-of-function mutations in SCN1b cause febrile seizures and generalised epilepsy (Wallace *et al.* 1998), but do not have a clear cardiac phenotype. In the brain there is very little overlap in the patterns of expression of SCN1b and SCN3b (Morgan *et al.* 2000). Conversely, both SCN1b and SCN3b are expressed in the ventricles and so it is possible that in these patients loss of SCN1b in the heart may be compensated for by the presence of SCN3b, at least in the ventricle. Many of the mutations of SCN5a associated with LQTS and Brugada syndrome appear to be modulated by co-expression of SCN1b (see, for example, An *et al.* 1998). To date, however, there are no reports of the effects of SCN3b on the phenotype of mutant SCN5a channels. One intriguing finding from our study is the lower density of α-subunit expression in the right ventricle compared to the left ventricle. This may contribute to the observation that many loss-of-function mutations of SCN5a are associated with more marked effects on the right side of the heart (Brugada *et al.* 2000).

An, R. H., Wang, X. L., Kerem, B., Benhorin, J., Medina, A., Goldmit, M. & Kass, R. S. (1998). Novel LQT-3 mutation affects Na^+ channel activity through interactions between alpha- and beta1-subunits. *Circulation Research* **83**, 141–146

Baroudi, G., Carbonneau, E., Pouliot, V. & Chahine, M. (2000). SCN5A mutation (T1620M) causing Brugada syndrome exhibits different phenotypes when expressed in *Xenopus* oocytes and mammalian cells. *FEBS Letters* **467**, 12–16.

Blount, P., Smith, M. M. & Merlie, J. P. (1990). Assembly intermediates of the mouse muscle nicotinic acetylcholine receptor in stably transfected fibroblasts. *Journal of Cell Biology* **111**, 2601–2611

Brugada, P., Brugada, R. & Brugada, J. (2000). Sudden death in high-risk family members: Brugada syndrome. *American Journal of Cardiology* **86**, K40–K43.

Catterall, W. A. (2000). From ionic currents to molecular mechanisms: the structure and function of voltage-gated sodium channels. *Neuron* **26**, 13–25.

Chen, Q., Kirsch, G. E., Zhang, D., Brugada, R., Brugada, J., Brugada, P., Potenza, D., Moya, A., Borggrefe, M., Breithardt, G., Ortiz-Lopez, R., Wang, Z., Antzelevitch, C., O'Brien, R. E., Schulze-Bahr, E., Keating, M. T., Towbin, J. A. & Wang, Q. (1998). Genetic basis and molecular mechanism for idiopathic ventricular fibrillation. *Nature* **392**, 293–296.

Ellgaard, L., Molinari, H. & Helenius, A. (1999). Setting the standards: quality control in the secretory pathway. *Science* **286**, 1882–1887

Gellens, M. E., George, A. L. Jr, Chen, L. Q., Chahine, M., Horn, R., Barchi, R. L. & Kallen, R. G. (1992). Primary structure and functional expression of the human cardiac tetrodotoxin-insensitive voltage-dependent sodium channel. *Proceedings of the National Academy of Sciences of the USA* **89**, 554–558.

Isom, L. L., De Jongh, K. S., Patton, D. E., Reber, B. F., Offord, J., Charbonneau, H., Walsh, K., Goldin, A. L. & Catterall, W. A. (1992). Primary structure and functional expression of the beta 1 subunit of the rat brain sodium channel. *Science* **256**, 839–842.

Isom, L. L., Ragsdale, D. S., De Jongh, K. S., Westenbroek, R. E., Reber, B. F., Scheuer, T. & Catterall, W. A. (1995). Structure and function of the beta 2 subunit of brain sodium channels, a transmembrane glycoprotein with a CAM motif. *Cell* **83**, 433–442.

Li, G.-R. & Shrier, A. (2001). Transmembrane sodium current is different in atrial from ventricular myocytes of guinea-pig heart. *Biophysical Journal* **80**, 189a.

Makita, N., Bennett, P. B. Jr & George, A. L. Jr (1994). Voltage-gated Na^+ channel beta 1 subunit mRNA expressed in adult human skeletal muscle, heart, and brain is encoded by a single gene. *Journal of Biological Chemistry* **269**, 7571–7578.

Malhotra, J. D., Chen, C., Rivolta, I., Abriel, H., Malhotra, R., Mattei, L. N., Brosius, F. C., Kass, R. S. & Isom, L. L. (2001). Characterization of sodium channel alpha- and beta-subunits in rat and mouse cardiac myocytes. *Circulation* **103**, 1303–1310.

Marban, E., Yamagishi, T. & Tomaselli, G. F. (1998). Structure and function of voltage-gated sodium channels. *Journal of Physiology* **508**, 647–657.

Morgan, K., Stevens, E. B., Shah, B., Cox, P. J., Dixon, A. K., Lee, K., Pinnock, R. D., Hughes, J., Richardson, P. J., Mizuguchi, K. & Jackson, A. P. (2000). Beta 3: an additional auxiliary subunit of the voltage-sensitive sodium channel that modulates channel gating with distinct kinetics. *Proceedings of the National Academy of Sciences of the USA* **97**, 2308–2313.

Nuss, H. B., Chiamvimonvat, N., Perez-Garcia, M. T., Tomaselli, G. F. & Marban, E. (1995). Functional association of the beta 1 subunit with human cardiac (hH1) and rat skeletal muscle (mu 1) sodium channel alpha subunits expressed in *Xenopus* oocytes. *Journal of General Physiology* **106**, 1171–1191.

Patel, M. K., Mistry, D., John, J. E. III & Mounsey, J. P. (2000). Sodium channel isoform-specific effects of halothane: protein kinase C co-expression and slow inactivation gating. *British Journal of Pharmacology* **130**, 1785–1792.

Priori, S. G. (2000). Long QT and Brugada syndromes: from genetics to clinical management. *Journal of Cardiovascular Electrophysiology* **11**, 1174–1178.

Qu, Y., Isom, L. L., Westenbroek, R. E., Rogers, J. C., Tanada, T. N., McCormick, K. A., Scheuer, T. & Catterall, W. A. (1995). Modulation of cardiac Na^+ channel expression in *Xenopus* oocytes by beta 1 subunits. *Journal of Biological Chemistry* **270**, 25696–25701.

Sakmann, B. F., Spindler, A. J., Bryant, S. M., Linz, K. W. & Noble, D. (2000). Distribution of a persistent sodium current across the ventricular wall in guinea pigs. *Circulation Research* **87**, 910–914.

Schott, J. J., Alshinawi, C., Kyndt, F., Probst, V., Hoorntje, T. M., Hulsbeek, M., Wilde, A. A., Escande, D., Mannens, M. M. & Le Marec, H. (1999). Cardiac conduction defects associate with mutations in SCN5A. *Nature Genetics* **23**, 20–21.

Stevens, E. B., Cox, P. J., Shah, B. S., Dixon, A. K., Richardson, P. J., Pinnock, R. D. & Lee, K. (2001). Tissue distribution and functional expression of the human voltage-gated sodium channel beta 3 subunit. *Pflügers Archiv* **441**, 481–488.

Sutkowski, E. M. & Catterall, W. A. (1990). Beta 1 subunits of sodium channels. Studies with subunit-specific antibodies. *Journal of Biological Chemistry* **265**, 12393–12399.

Wallace, R. H., Wang, D. W., Singh, R., Scheffer, I. E., George, A. L. Jr, Phillips, H. A., Saar, K., Reis, A., Johnson, E. W., Sutherland, G. R., Berkovic, S. F. & Mulley, J. C. (1998). Febrile seizures and generalized epilepsy associated with a mutation in the Na^+-channel beta1 subunit gene SCN1B. *Nature Genetics* **19**, 366–370.

Wang, Q., Shen, J., Splawski, I., Atkinson, D., Li, Z., Robinson, J. L., Moss, A. J., Towbin, J. A. & Keating, M. T. (1995). SCN5A mutations associated with an inherited cardiac arrhythmia, long QT syndrome. *Cell* **80**, 805–811.

Watanabe, T., Rautaharju, P. M. & McDonald, T. F. (1985). Ventricular action potentials, ventricular extracellular potentials, and the ECG of guinea pig. *Circulation Research* **57**, 362–373.

Wong, K. R., Trezise, A. E., Bryant, S., Hart, G. & Vandenberg, J. I. (1999). Molecular and functional distributions of chloride conductances in rabbit ventricle. *American Journal of Physiology* **277**, H1403–1409.

Acknowledgements

We gratefully acknowledge Al George Jr and Lori Isom for supplying the cDNAs and antibodies. J.I.V. is a British Heart Foundation Basic Sciences Lecturer, and A.P.J. thanks the Wellcome Trust for financial support.

Corresponding author

J. I. Vandenberg: Victor Chang Cardiac Research Institute, Level 9, 384 Victoria Street, Darlinghurst, NSW 2010, Australia.

Email: j.vandenberg@victorchang.unsw.bde.au

Author's present address

E. B. Stevens: Cambridge Drug Discovery, 10 Science Park, Cambridge CB4 0FG, UK.